

Quantification of Saccharides in Multiple Floral honeys Using Fourier Transform Infrared Microattenuated Total Reflectance Spectroscopy

JAGDISH TEWARI AND JOSEPH IRUDAYARAJ*

227 Agricultural Engineering Building, Department of Agricultural and Biological Engineering,
 The Pennsylvania State University, University Park, Pennsylvania 16802

Fourier transform infrared (FTIR) spectroscopy with microattenuated total reflectance (mATR) sampling accessory and chemometrics (partial least squares and principal component regression) was used for the simultaneous determination of saccharides such as fructose, glucose, sucrose, and maltose in honey. Two calibration models were developed. The first model used a set of 42 standard mixtures of fructose, glucose, sucrose, and maltose prepared over the range of concentrations normally present in honey, whereas the second model used a set of 45 honey samples from various floral and regional sources. The developed models were validated with different data sets and verified by high-performance liquid chromatography (HPLC) measurements. The R^2 values between the FTIR-mATR predicted and HPLC results of the different sugars were between 0.971 and 0.993, demonstrating the predictive ability and accuracy of the procedure.

KEYWORDS: FTIR; ATR; chemometrics; HPLC; rapid; sugars

INTRODUCTION

The primary constituents of honey are fructose (38%), glucose (31%), moisture (17%), maltose (7%), and sucrose (1%). Other components present in minute quantities include organic acids, amino acids, enzymes, vitamins, flavonoids, and acetylcholine, which give honey its color, flavor, and aroma. Although the minor components of honey combined contribute only very little to the total mass, these trace elements give honey its unique characteristics and consumer appeal. It should also be noted that honey from the same floral source might differ in composition due to seasonal, climatic, or geographical variations. A combination of the floral type, seasonal, and geographical factors makes it very difficult to standardize the composition of honey and to assign specific quality attributes. The composition details from a survey (1) of ~490 samples of honey presented in **Table 1** indicate that the primary sugars, glucose and fructose, account for ~65–85% of the total carbohydrate content (2) in honey.

A variety of chromatographic methods such as paper chromatography (3), high-performance liquid chromatography (HPLC), thin-layer chromatography (4, 5), gas–liquid chromatography (6), and HPEA-PAD (7) have been used to measure the concentration of different saccharides in honey. Vibrational spectroscopy has also been used to quantify the carbohydrate content in honey (8).

Arboleda and Lopponow applied Raman spectroscopy to characterize a mixture of carbohydrates present in unknown sugar samples (9). Fourier transform Raman spectra of several

Table 1. Average Composition of Honey

component	av	SD	range
moisture (%)	17.2	1.46	13.4–22.9
fructose (%)	38.19	2.07	27.25–44.26
glucose (%)	31.28	3.03	22.03–40.73
sucrose (%)	1.31	0.95	0.25–7.57
maltose (%)	7.31	2.09	2.74–15.98
higher sugar (%)	1.50	1.03	0.13–8.49
lactone, mequiv/kg	0.335	0.13	0.0–0.95
ash (%)	0.169	0.15	0.02–1.028
proteins, amino acids, vitamins, and minerals	0.50		
total acid (gluconic acid)	0.57	0.20	0.17–1.17
nitrogen	0.041	0.026	0.000–0.133
pH	3.91		3.42–6.10
diastase value	20.8	9.8	2.1–61.2

commercial samples of honey showed that the relative intensities of the vibration bands in the C–H stretching region of the FT Raman spectra are sensitive to the observed physical states of the specimen (10). Transmittance near-infrared spectra has also been used for composition assessment (11) because several vibrational bands related to fructose and glucose could be observed in the 500–1800 cm^{-1} fingerprint region.

The suitability of Fourier transform infrared attenuated total reflectance (FTIR-ATR) spectroscopy as an analytical technique in food analysis has been investigated because it is a fast and nondestructive alternative to conventional methods. Generally, one of the several multivariate methods such as the partial least-squares (PLS) and/or principal component regression (PCR) is used to develop prediction models for multicomponent analysis

* Corresponding author [telephone (814) 865-2807; fax (814) 863-1031; e-mail josephi@psu.edu].

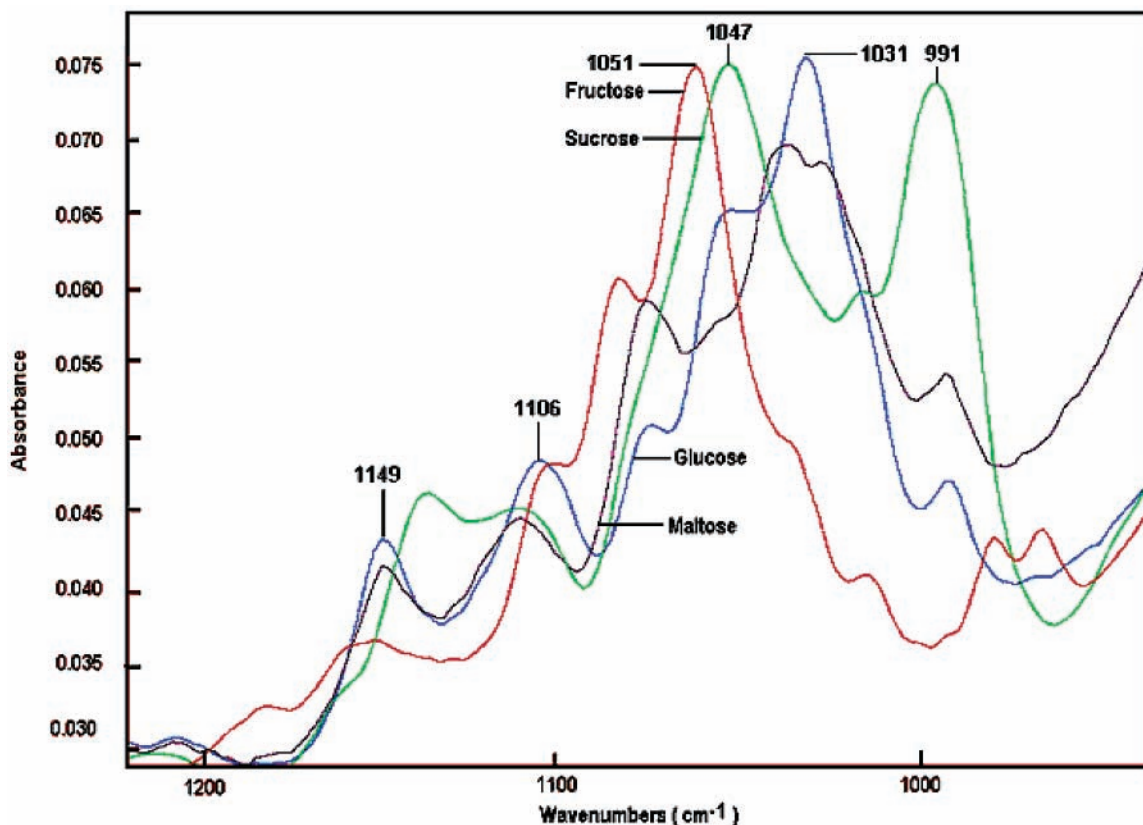


Figure 1. Overlaid FTIR-mATR spectra of honey constituents.

(12–15). A comparative study of the different multivariate calibration methods by Dupay et al. (16) to determine glucose, fructose, and sucrose levels in dried fruit juice extracts showed that PLS is a better predictor than PCR. Multivariate analysis is often used to extract subtle information from complex spectra that might contain overlapping peaks, interference bands due to water or carbon dioxide, and instrumental artifacts due to measurement conditions (17). Several applications of FTIR spectroscopy to detect the presence of beet and cane invert sugars in purposefully adulterated honey show the potential of this technique as a rapid tool to quantify and monitor the major sugar components in honey (18, 19).

In this work, we have reported for the first time a rapid and nondestructive FTIR- micro-ATR spectroscopic approach for the simultaneous prediction of glucose, fructose, sucrose, and maltose in honey samples obtained from around the world. Calibration models developed using PLS and PCR methods were validated with HPLC measurements of all honey samples tested.

EXPERIMENTAL PROCEDURES

Preparation of Standard Mixtures. Forty-two standard sugar mixtures with known concentrations of glucose (22–40%), fructose (22–44%), sucrose (0.25–7.5%), and maltose (2.75–15%) were carefully prepared in the range of concentrations present in natural honey (Table 1). Ten independent samples of random sugar mixtures were separately prepared for validation and are presented in Table 3.

Honey Samples. More than 50 different types of honeys from different floral sources (Table 5) were obtained through the National Honey Board (Longmont, CO) from different sources and used for calibration as well as validation.

FTIR-mATR Measurement. FTIR measurements were carried out with a Bio-Rad 3000 Excalibur spectrometer with an mATR sampling accessory from Pike Technologies (Madison, WI). The spectrometer is equipped with a deuterated triglycine sulfate (DTGS) detector, operating at 4 cm^{-1} resolution and 0.32 cm/s mirror velocity. Two

hundred and fifty-six interferograms were co-added before Fourier transformation. The instrument was allowed to purge for 5 min with nitrogen gas (grade1) prior to acquisition of the spectra to minimize the spectral contribution due to atmospheric carbon dioxide and water vapor. The mATR-MIRacle cell sampling accessory has a single-bounce horizontal ATR (HATR) zinc selenide (ZnSe) crystal 1.5 mm in diameter and a refractive index of 2.34 designed for use in the FTIR spectrometer. The depth of penetration of the infrared beam is 1.46 μm . A major advantage of this accessory is that it requires smaller sample volumes (~0.5 mL) compared to the multiple-bounce HATR accessory; however, the single-bounce accessory is less sensitive because of the decreased signal contact with the sample.

Single-beam spectra of all the samples were obtained and ratioed against the background spectrum of air to present the spectra in absorbance units. The spectrum of the blank mATR-MIRacle cell was used as reference. After every measurement, the mATR crystal was thoroughly washed with distilled water and dried, and its spectrum was examined to ensure that sample residues from the previous acquisition were not retained on the crystal surface. Each experiment was replicated three times.

Chemometrics. The GRAMS 32 (Galactic Industries Corp., Salem, NH) software package was used for quantitative analysis by PLS (20) and PCR (21). PLS, a quantitative spectral decomposition technique, uses the concentration information during the decomposition process. This causes the spectra of the samples with higher constituent concentration to be weighted more heavily than samples with lower concentrations. The main idea of PLS is to account for as much concentration information as possible in the first few loading vectors. The PCR method combines the principal component analysis (PCA) spectral decomposition with an inverse least squares (ILS) regression method to develop a quantitative model for complex samples, whereas the PCR method regresses the concentrations with the PCA scores.

In this research calibration models were developed using PLS/IQ to predict the unknown sugar concentration on the basis of the information contained in the spectra. The undesirable variations in the spectra were removed using the mean center and autobaseline methods. The training sets were built with PLS and PCR calibration and cross-validation

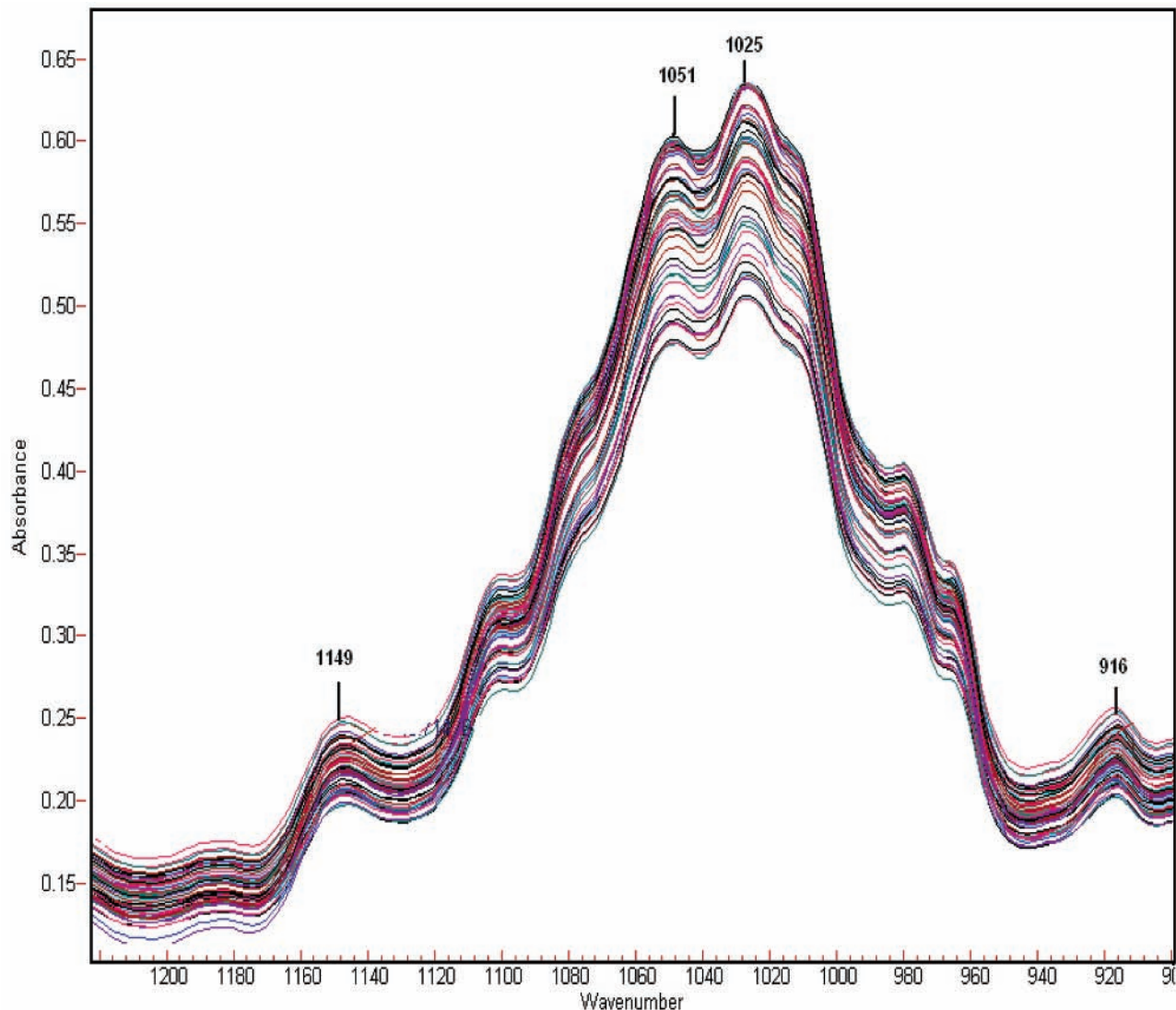


Figure 2. FTIR-mATR spectra of a mixture of sucrose, glucose, fructose, and maltose.

diagnostics, using three files out of rotation. Factors for the models were obtained by the leave-one-cross-validation technique based on the minimum predicted residual sum of squares (PRESS) and an optimum R^2 value, which should be as high as possible. The predictive ability of the models was tested by computing the standard error of calibration (SEC) and the standard error of prediction (SEP) presented by

for calibration data

$$SEC = \sqrt{\frac{\sum_{i=1}^n (\text{actual} - \text{predicted})^2}{n - f - 1}}$$

for validation data

$$SEP = \sqrt{\frac{\sum_{i=1}^n (\text{actual} - \text{predicted})^2}{n}}$$

The term “actual” refers to the concentration of sugars in the aqueous mixture, and “predicted” refers to the concentration value computed by PCR/PLS from the sample spectra; n is the number of samples in the calibration set, and f refers to the number of factors in the calibration

Table 2. Functional Groups and Vibrational Modes of Honey from the FTIR Spectra

wavenumber (cm ⁻¹)	vibrational group	vibrational mode
927	C—H (carbohydrates)	bending
991	C—O (C—OH)	stretching
1042	C—O (C—OH)	stretching
	C—O (C—OH)	stretching
1110	C=O of ketones	stretching/bending
	C=O (C—O—C bond)	stretching/bending
1259	C—O (C—OH)	stretching
1327	O—H (C—OH)	stretching/bending
1419	O—H (C—OH)	stretching/bending

model. Cross-validation was used in all cases to minimize the risk of overfitting when calibration accuracy was evaluated.

High-Performance Liquid Chromatography. HPLC measurements were done using the Waters HPLC system (Franklin, MA) equipped with an autosampler, UV detector, column heater, and controller with sulfuric acid as the mobile phase. Calibration was first done using standard solutions of sucrose, glucose, fructose, or maltose before actual measurement. For quantification of the components at higher concentrations, samples were appropriately diluted for analysis. Separation of glucose, fructose, sucrose, and maltose in the honey samples was carried out using an Aminex HPX-87H (300 × 7.8 mm) and a fast carbohydrate column (100 × 7.8 mm). The flow rate was kept at 0.6 mL/min for HPX-87H and at 1.2 mL/min for the fast carbohydrates column to

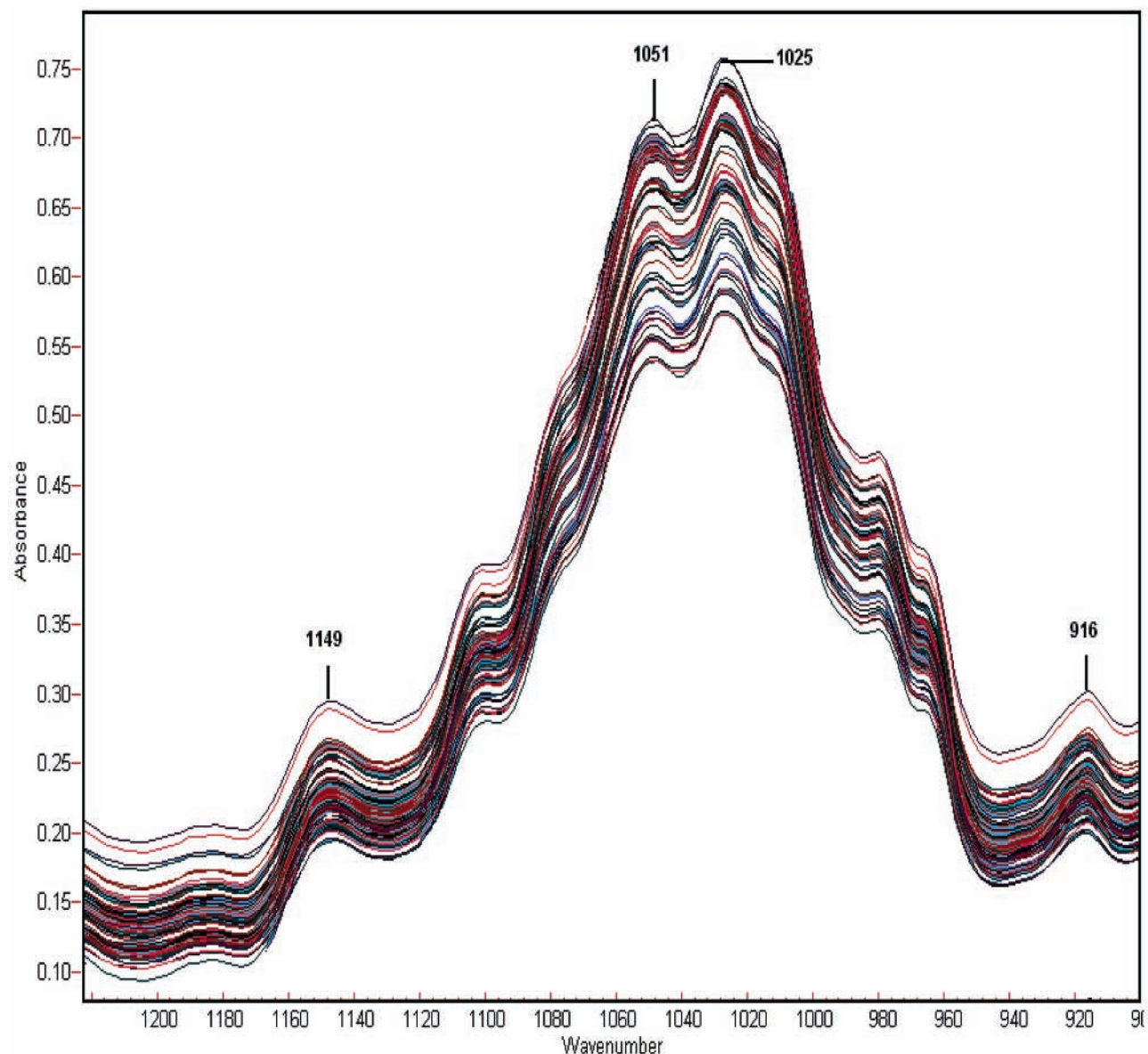


Figure 3. Overlaid FTIR-mATR spectra of various worldwide honey samples.

Table 3. Predicted Concentration of Saccharides in the Validation Set of Synthetic Samples by PLS and PCR^a

fructose (%)			glucose (%)			sucrose (%)			maltose (%)		
AConcn	PLSp	PCRp	AConcn	PLCp	PCRp	AConcn	PLSp	PCRp	AConcn	PLSp	PCRp
27.0	26.2	25.7	22.0	22.5	20.9	2.0	2.5	3.0	4.0	4.5	5.0
27.5	27.0	26.0	23.1	23.7	22.3	2.5	3.0	3.2	5.0	5.6	6.0
28.0	27.7	28.6	25.3	25.9	24.3	3.0	3.5	2.6	6.0	5.6	4.2
28.5	29.0	27.1	27.4	26.9	26.1	2.3	2.6	3.0	7.0	7.7	7.4
29.5	30.2	28.0	29.6	29.0	29.0	3.5	3.9	3.0	8.0	8.3	8.4
31.0	30.0	31.6	30.8	30.1	30.6	3.7	4.2	3.5	9.0	9.6	9.9
32.0	32.6	31.1	31.0	31.5	32.0	4.0	3.5	5.0	10.0	10.0	10.6
33.0	33.4	34.5	32.4	32.5	32.9	4.2	4.5	4.0	1.0	11.6	10.9
35.0	35.6	37.1	33.6	34.0	35.0	5.0	5.6	4.1	11.5	11.2	12.3
36.0	36.5	36.2	34.0	34.2	35.0	5.5	6.0	6.5	12.0	12.3	12.4

^a AConcn, actual concentration; PLSp, partial least-squares prediction; PCRp, principal component regression prediction.

prevent baseline drift. Triplicate injections were carried out to ensure accurate estimation of the sugars measured.

Models Developed. Two different calibration models were developed to predict the concentrations of the different sugars in honey. The first model was developed with data from the 42 synthetic sugar mixture samples of known concentrations and validated by predicting the sugar concentrations in 10 synthetic sugar samples prepared separately as well as 45 different honey samples. The second model was developed

from the HPLC-measured sugar concentrations in 45 different honey samples and validated against 15 other honey samples.

RESULTS AND DISCUSSION

Figure 1 shows the overlaid spectra of sucrose, glucose, fructose, and maltose in pure solutions. The spectral region between 750 and 1500 cm^{-1} corresponds to the absorption

Table 4. Calibration and Validation Statistics^a for the Models Developed with Data from 42 Sugar Mixtures and 45 Honey Samples

chemometrics	reference method, model from	analysis factors	calibration		validation	
			R ²	SEC	R ²	SEP
PLS	sugar mixture data	6	0.998	0.662	0.958	1.8
PCR	sugar mixture data	5	0.898	0.671	0.928	2.1
PLS	honey samples	6	0.997	0.656	0.955	1.2
PCR	honey samples	5	0.965	0.668	0.927	1.5

^a SEC, standard error of calibration; SEP, standard error of prediction; R², correlation coefficient.

region of the sugars and higher sugars analyzed. The region 750–900 cm⁻¹ corresponds to the anomeric region characteristic of the saccharide configuration (22). The bands in the 904–1153 cm⁻¹ region are assigned to C–O and C–C stretching modes (23), and those around 1199–1474 cm⁻¹ could be due to the bending modes of O–C–H, C–C–H, and C–O–H. Negative bands observed around 1618 and 3635 cm⁻¹ are due to lower water concentration in honey, because water presents an O–H stretching band around these regions (24).

The peak at 927 cm⁻¹ may be due to the C–H bending of carbohydrate, whereas the peaks observed at 991, 1042, 1106, and 1259 cm⁻¹ may be due to the C–O stretch in the C–OH group as well as the C–C stretch in the carbohydrate structure. In addition, the peak at 1110 cm⁻¹ may be due to stretching of the C–O bond of the C–O–C linkage. The C–O–C is present in sucrose as a glycosidic bond, a band linking monosaccharides such as glucose and fructose. The peak around 1327 cm⁻¹ may be due to O–H bending of the C–OH group, and the band at 1419 cm⁻¹ may be due to a combination of O–H bending of the C–OH group and C–H bending of alkenes. Key functional groups and their vibrational mode are presented in **Table 2**.

As a first step in the spectral region selection for quantitative estimation of fructose, glucose, sucrose, and maltose in various worldwide honey samples, the wavelength range in which absorbance measurement should be made needs to be determined. When latent methods such as PLS and PCR are employed to develop calibration models, the spectral range dictates the number of spectral points used in the computation of latent variables. The spectral range should include charac-

Table 5. Comparison of FTIR-PLS Sugar Mixture Model Predictions with HPLC Results

honey	fructose (%)		glucose (%)		sucrose (%)		maltose (%)	
	FTIR	HPLC	FTIR	HPLC	FTIR	HPLC	FTIR	HPLC
Christmas, FL	39.21	39.29	28.00	28.90	5.54	5.44	10.26	10.30
mesquite	36.22	36.15	27.21	27.32	6.69	6.66	11.25	11.32
blackberry, NC	38.22	38.30	25.32	25.30	3.12	3.20	8.35	8.400
tallow, TX	38.22	38.40	29.12	29.10	4.55	4.22	7.69	7.740
tarweed, CA	37.55	37.67	30.25	30.20	6.00	6.02	8.69	8.710
clover, Canada	35.23	36.41	23.54	24.52	5.19	5.20	9.60	9.630
China ELA	39.24	39.33	26.12	26.21	3.00	3.21	10.25	10.32
carrot	37.32	37.45	26.22	26.20	3.10	3.21	9.22	9.32
Chile	33.65	33.62	24.58	24.56	5.32	5.32	12.39	12.50
Brazilian orange	38.87	38.61	30.34	30.34	4.00	4.32	11.57	11.50
Indian	36.54	36.00	29.21	29.32	5.35	5.32	10.25	10.32
Australian tallow	35.87	35.67	26.20	26.40	4.36	4.32	13.25	13.20
Canada WH clover	36.68	36.10	27.21	27.12	5.69	5.71	10.36	10.33
Uruguay	36.63	36.99	28.36	28.35	3.25	3.21	12.68	12.70
kiwi	38.62	38.51	33.21	33.10	5.65	5.63	8.56	8.62
tallow harden, TX	36.62	36.42	26.25	26.30	6.36	6.40	10.00	10.12
alfalfa, CA	39.12	39.12	28.26	28.20	3.20	3.10	7.26	7.23
alfalfa, UT	38.79	38.88	30.13	30.21	5.63	5.21	11.58	11.43
eucalyptus, Canada	37.32	37.21	30.11	30.13	5.31	5.20	10.22	10.21
buckwheat, NM	36.54	36.40	29.54	29.32	3.22	3.21	10.88	10.60
cotton, CA	35.84	35.71	27.14	27.20	4.42	4.30	13.93	13.76
melter, CA	36.81	36.36	25.45	25.30	4.65	4.26	10.12	10.57
mint, ID	36.31	36.40	28.23	28.60	3.23	3.10	12.10	12.26
sourwood, WA	33.12	33.25	39.11	39.60	4.01	4.00	8.60	8.62
tropical blossom	36.12	36.10	28.21	28.90	5.45	5.20	8.65	8.55
blueberry, ME	33.14	33.20	32.21	32.20	3.15	3.21	9.54	9.24
Polk tupelo, FL	35.25	35.00	25.54	25.50	5.23	5.24	11.00	11.03
gallberry, CA	36.14	36.51	32.12	32.65	3.90	3.54	6.30	6.25
eucalyptus, CA	38.32	38.49	35.32	35.40	3.25	3.23	7.69	7.69
basswood, NY	35.22	35.00	25.32	25.30	3.65	3.21	11.56	11.32
basswood, Canada	34.55	34.40	25.23	25.20	3.22	3.34	10.21	10.32
mesquite, CA	36.40	36.65	31.12	31.26	2.37	2.53	6.39	6.35
clover, ND	36.32	36.96	30.12	30.26	2.33	2.36	6.50	6.58
clover, FL	35.22	35.65	30.22	30.21	3.57	3.54	5.73	5.69
buckwheat, TX	36.43	36.49	31.10	31.21	4.32	4.54	6.54	6.71
Turkey ELA	35.42	35.36	32.44	32.84	4.71	4.65	8.65	8.55
Mexican ELA	36.32	36.52	32.43	32.33	5.35	5.32	8.56	8.64
blueberry, ME	33.25	33.20	32.12	32.20	3.11	3.21	9.14	9.24
tupelo, FL	35.12	35.00	25.15	25.50	5.30	5.24	11.10	11.00
China ELA	39.24	39.33	26.11	26.21	3.25	3.21	10.39	10.32
mint, LA	36.12	36.22	32.35	32.45	5.90	5.98	10.59	10.54
Chile	33.56	33.62	24.43	24.56	5.42	5.32	12.57	12.50
blackberry, NC	38.21	38.30	25.23	25.30	3.11	3.20	8.50	8.40
tallow, TX	37.93	37.87	30.23	30.21	4.3	4.9	8.70	8.90
orange blossom	35.32	35.67	31.22	32.00	5.4	5.0	9.10	9.89

R² = 0.971R² = 0.993R² = 0.972R² = 0.992

Table 6. Comparison of FTIR-PLS Model Developed from the Spectra of Honey Samples Model with HPLC Measurements of the Validation Set

honey	fructose (%)			glucose (%)			sucrose (%)			maltose (%)		
	HPLC	PLSp	PCRp	HPLC	PLCp	PCRp	HPLC	PLSp	PCRp	HPLC	PLSp	PCRp
clover, MA	35.1	35.2	35.4	33.1	33.2	33.4	2.4	2.5	2.3	6.8	7.1	6.9
alfalfa, CA	36.1	36.4	36.5	30.1	30.6	31.2	2.4	2.6	2.4	8.1	8.3	7.5
carrot, LA	34.1	34.7	34.5	31.1	31.3	31.7	3.0	3.1	3.4	7.4	7.5	7.1
wildflower, PA	33.5	33.6	33.8	32.7	32.5	32.9	3.2	3.6	3.5	6.4	6.7	6.5
wildflower, CA	34.0	34.8	34.2	33.4	33.2	33.3	4.3	4.4	4.6	5.9	6.1	5.9
mint, NY	35.9	35.8	35.7	34.2	34.5	33.9	1.2	1.4	1.5	6.6	6.7	6.9
buckwheat	36.3	36.2	36.8	33.3	33.2	33.6	2.1	2.5	2.2	7.4	7.6	7.7
soybean, CA	34.2	34.1	34.5	32.5	32.9	32.9	3.0	3.5	3.6	5.7	5.4	5.7
sourwood	38.6	38.6	38.5	35.4	34.9	36.6	3.2	3.5	3.5	5.6	5.3	5.5
sunflower FL	36.2	36.4	36.6	30.1	30.1	30.8	3.4	3.6	4.1	6.7	6.9	6.3
wildflower, Argentina	35.3	35.6	35.7	32.3	32.3	32.9	2.2	2.4	2.3	7.5	7.6	7.3
tallow, China	33.2	33.4	33.6	31.2	31.3	31.5	2.3	2.6	2.5	6.9	6.9	6.6
house mint, TX	36.3	36.6	36.5	32.5	32.2	32.9	2.3	2.5	2.0	7.6	7.4	7.1
multifloral, Mexico	36.3	36.5	36.0	31.3	30.6	31.5	3.6	3.5	3.5	8.6	8.5	8.5
goldenrod ELA, USA	36.2	36.4	36.4	34.3	34.6	34.6	3.2	3.0	3.0	7.5	7.6	7.4

$R^2 = 0.972$ (PLS)
 $R^2 = 0.970$ (PCR)

$R^2 = 0.953$ (PLS)
 $R^2 = 0.935$ (PCR)

$R^2 = 0.941$ (PLS)
 $R^2 = 0.897$ (PCR)

$R^2 = 0.954$ (PLS)
 $R^2 = 0.904$ (PCR)

teristic regions in which the chemical groups related to the species of interest as well as other matrix constituents absorb. Most ideally, regions dominated by noise or other artifacts should not be included in the analysis. Although this may not be entirely possible when absorptions due to artifacts and analytes overlap, even minor considerations will help in developing a robust model. A suitable spectral range can be identified by computing the correlation spectrum for the constituents of interest by calculating the correlation of absorbance at every wavelength or wavenumber in the spectra against the concentration of sugars. Regions that show a high positive or negative correlation are ranges that should be selected, whereas regions that show low or no correlation should be ignored. Due to the presence of sugars in honey, the region between 600 and 1400 cm^{-1} had the highest correlation as expected and, hence, was selected for calibration.

Figure 2 depicts the family of spectra from the sugar mixture samples used for calibration model development (model 1). **Figure 3** indicates that the spectra of the various honey samples analyzed were identical. Results of the PLS and PCR predictions for the 10 sugar mixture samples in the validation set are presented in **Table 3**. The R^2 , SEC, and SEP values for all of the sugars assessed show that the PLS model is a better predictor compared to the PCR model with a lower SEP and a higher R^2 value (**Table 4**). The calibration model developed from the sugar mixture spectra was further verified by testing its glucose, fructose, sucrose, and maltose prediction accuracy in different honey samples. HPLC measurements of the different sugars are compared with the FTIR-PLS model predictions and presented in **Table 5**. The difference in the concentration of sugars in the various honey samples demonstrates that there are concentration differences in the nectar and pollen of the different types of honey examined.

Table 4 also presents the R^2 , SEC, and SEP values for the second calibration model developed from the 45 honey samples as determined by HPLC measurements. The calibration model was then validated by an external set of 15 honey samples (**Table 6**). The HPLC measurements of fructose, glucose sucrose, and maltose were almost similar to the FTIR predictions presented in **Table 6**. The correlation values (R^2) for all sugars between the HPLC and FTIR predictions were between 0.971 and 0.993, demonstrating that the procedure adopted could be used for rapid and simultaneous measurement of the different sugars studied.

The infrared technique can be a suitable method for the simultaneous and rapid determination of sucrose, glucose, fructose, and maltose in honey. The models developed using synthetic mixtures as well as real honey samples showed a high correlation; however, calibration models developed from the spectra of honey samples were better because the contributions of components other than the sugars were also incorporated in the calibration. The important characteristics of the present study are that the components of honey can be determined simultaneously in <5 min without any physical or chemical manipulation.

LITERATURE CITED

- (1) White, J. W.; Riethof, M. L.; Subers, M. H.; Kushnir, I. Composition of American honey, Washington, DC: Agricultural research service. *USDA Tech. Bull.* **1962**, No. 1261, 12–18.
- (2) White, J. W. Composition of honey. In *Honey: A Comprehensive Survey*; Crane, E., Ed.; London, U.K., 1975; pp 157–61.
- (3) Partridge, S. M. Aniline Hydrogen Phthalate as a spraying reagent for chromatography of sugars. *Nature* **1949**, *164*, 443.
- (4) Honda, S. High performance liquid chromatography of monosaccharide and oligosaccharides. *Anal. Biochem.* **1984**, *140*, 1–47.
- (5) Tate, M. E.; Bishop, C. T. Thin-layer chromatography of carbohydrate acetates. *Can. J. Chem.* **1962**, *40*, 1043–1048.
- (6) Merker, H. M.; Beecher, G. R. Measurement of food flavonoids by high-performance liquid chromatography: A Review. *J. Agric. Food Chem.* **2000**, *48*, 577–599.
- (7) Valoran, P. H.; Jeffrey, S. R. Determination of Carbohydrates, Sugar Alcohols, and Glycols in Cell Cultures and Fermentation Broths Using High-Performance Anion-Exchange Chromatography with Pulsed Amperometric Detection. *Anal. Biochem.* **2000**, *283*, 192–199.
- (8) Vasko, P. D.; Blackwell, J.; Koenig, J. L. Infrared and Raman spectroscopy of carbohydrates part I. Identification of O–H and C–H related vibrational modes for D-glucose, maltose, cellobiose and dextran by deuterium-substitution methods. *Carbohydr. Res.* **1971**, *19*, 297–310.
- (9) Arboleda, P. H.; Loppnow, G. R. Raman Spectroscopy as a discovery tool in carbohydrate chemistry. *Anal. Chem.* **2000**, *72*, 2093–2098.
- (10) Fernando, L.; Oliveira, C.; Colombara, R.; Edwards, H. G. M. Fourier transform Raman spectroscopy of honey. *Appl. Spectrosc.* **2002**, *56* (3), 306–310.
- (11) Qui, P. Y.; Ding, H. B.; Xu, R. J. Determination of chemical composition of commercial honey by near-infrared spectroscopy. *J. Agric. Food Chem.* **1999**, *47*, 2760–2765.

- (12) Kemsely, E. K.; Zhou, L.; Hammouri, M. K.; Wilson, R. H. Quantitative analysis of sugar solution using infrared spectroscopy. *J. Food Chem.* **1992**, *44*, 304–309.
- (13) Picque, D.; Lefier, D.; Grappin, R.; Corrieu, G. Monitoring of fermentation by infrared spectroscopy-alcoholic and lactic fermentations. *Anal. Chem. Acta* **1993**, *279*, 67–72.
- (14) Cadit, F.; Offmann, B. Extraction of characteristic bands of sugars by multidimensional analysis of their infrared spectra. *Spectrosc. Lett.* **1996**, *29*, 523–536.
- (15) Sivakesava, S.; Irudayaraj, J. Determination of sugars in aqueous mixtures using mid-infrared spectroscopy. *J. Appl. Eng. Agric.* **2000**, *16*, 543–550.
- (16) Dupay, N.; Meurens, Somberet, M. B.; Legrand, P.; Huvenne, J. P. Determination of sugars and organic acids in fruit juices by FT Mid-IR investigation of dry extract. *Appl. Spectrosc.* **1992**, *46*, 860–863.
- (17) Beebe, K. R.; Pell, R. J.; Seasholtz, M. B. *Chemometrics—A Practical Guide*; Wiley: New York, 1998; p 186.
- (18) Sivakesava, S.; Irudayaraj, J. Detection of inverted beet sugar adulteration of honey by FTIR spectroscopy. *J. Sci. Food Agric.* **2001**, *81*, 683–690.
- (19) Sivakesava, S.; Irudayaraj, J. Prediction of inverted cane sugar adulteration of honey by Fourier transform infrared spectroscopy. *J. Food Sci.* **2001**, *66*, 972–978.
- (20) Haaland, D. M.; Thomos, E. V. Partial least squares methods for spectral analyses: Relations to other quantitative calibration methods and the extraction of qualitative calibration information. *Anal. Chem.* **1988**, *60*, 1193–1202.
- (21) Martens, H.; Naes, T. *Multivariate Calibration: Assessment, Validation and Choice of Calibration Method; Pretreatment and Linearization*; Wiley: Chichester, U.K., 1988; pp 116–165.
- (22) Tul'chinsky, V. M.; Zurabian, S. F.; Asankozhoev, K. A.; Kogan, G. A.; Khorlin, A. Y. Study of infrared spectra of oligosaccharides in the region 1000–400 cm⁻¹. *Carbohydr. Res.* **1976**, *51*, 1–15.
- (23) Hineno, M. Infrared spectra and normal vibrations of β -D-glucopyranose. *Carbohydr. Res.* **1977**, *56*, 219–223.
- (24) Chen, M.; Irudayaraj, J. Sampling technique for cheese analysis by FTIR spectroscopy. *J. Food Sci.* **1998**, *63*, 96–99.

Received for review October 13, 2003. Revised manuscript received April 4, 2004. Accepted April 11, 2004. We gratefully acknowledge funding from The National Honey Board (Longmont, CO) to support this research.

JF035176+